

Title no. 85-S35

## Drop, Fire, and Thermal Testing of a Concrete Nuclear Fuel Container



by Frank J. Vecchio and James A. Sato

*Describes the structural testing performed on two half-scale models of a concrete cask proposed as a container for irradiated nuclear reactor fuel. The testing conducted on the first model was based on International Atomic Energy Agency (IAEA) regulations for licensing containers used to transport high level radioactive materials. The tests consisted of a drop test from a height of 9 m (30 ft), followed by a 1-m (3.3-ft) drop onto a steel pin, followed by exposure to a severe fire condition. The second model was subjected to tests representing thermal loads encountered under normal service conditions.*

*The cask models withstood all test conditions, retaining their structural integrity and providing full containment of the simulated payload. Significant cracking, spalling and crushing of concrete, and rupturing of reinforcing bars were experienced, however. The test program and the results are discussed herein, with emphasis on aspects pertaining to structural performance.*

**Keywords:** containment; conveying; density (mass/volume); fire tests; fuels; high-strength concretes; impact tests; irradiation; nuclear reactors; radiation shielding; reinforced concrete; storage; thermal gradient; wastes; weathering.

A need exists for long-term solutions to the problem of safe handling and final disposal of irradiated nuclear reactor fuel. Currently, work is directed towards developing alternative programs for irradiated fuel management (IFM), where such programs must make provisions for interim on-site storage, for off-site transportation, and for final disposal of the irradiated fuel. While current IFM strategies are typically based on the use of three distinct handling and containment systems, the possibility of using one container for all three aspects of IFM is also being examined. In this respect, reinforced concrete is being recognized as a potentially viable material for use in the fabrication of such integrated containers.

Prototype containers must be shown to meet a number of stringent performance criteria, including radiation shielding requirements, long-term material stability, and structural integrity. For transporting high-level waste, a highly regulated activity, the International Atomic Energy Agency (IAEA) requires that a proto-

type cask be licensed by subjecting a model to two successive drop tests followed by thermal radiation exposure (i.e., fire test). The drop tests, in particular, impose severe demands on the structural integrity and containment value of the package and, thus, often represent the severest test of the viability of any integrated IFM system.

A comprehensive program was initiated at Ontario Hydro with the aim of developing and assessing the performance of a concrete integrated container or concrete cask as a possible IFM option. An essential aspect of the developmental program involved the fabrication of two half-scale models of a prototype cask. One model was subjected to drop and fire tests as per IAEA guidelines. The second was subjected to various thermal environments which would be expected in the storage phase of an integrated IFM plan. The test program and test results will be discussed in this paper. The scope of the discussion is limited to aspects pertaining only to structural performance under the imposed load conditions.

### RESEARCH SIGNIFICANCE

The reinforced concrete cask models tested were subjected to extreme impact, puncture, and fire conditions, as well as simulated service conditions. Few experimental data have been previously reported in this regard, particularly for high-density concrete. The casks' performance, both from measured data and visual observation, will assist in understanding the behavior of reinforced concrete containers under severe load conditions and may point to methods of improving current cask designs.

Received Sept. 9, 1986, and reviewed under Institute publication policies. Copyright © 1988, American Concrete Institute. All rights reserved, including the making of copies unless permission is obtained from the copyright proprietors. Pertinent discussion will be published in the May-June 1989 *ACI Structural Journal* if received by Jan. 1, 1989.

ACI member Frank J. Vecchio is an assistant professor in the Department of Civil Engineering at the University of Toronto, Ontario, Canada. He is on a leave of absence from Ontario Hydro, where he was involved in the analysis and design of reinforced concrete nuclear power plant structures. Dr. Vecchio is a member of ACI Committee 435, Deflection of Concrete Building Structures, and of Canadian Standard Association CSA-N287.3, Technical Committee on Concrete Containment Structures for Nuclear Power Plants.

ACI member James A. Sato is a research engineer at Ontario Hydro. A graduate from the University of Toronto, his research at Ontario Hydro is related to the design and development of reinforced concrete nuclear containment systems and structures.

## CONCRETE CASK TECHNOLOGY

Concrete is an effective and relatively inexpensive shielding material, making the concept of concrete casks viable for use in packaging nuclear wastes. Developmental work in Canada began in 1974 with a test program by Atomic Energy of Canada Ltd. (AECL)<sup>1</sup> aimed at evaluating the performance of concrete storage casks. A subsequent test program<sup>2</sup> investigated extending the function of the concrete casks from storing to transporting irradiated fuel. The results revealed that normal density reinforced concrete casks would have difficulties passing the impact and puncture conditions experienced in the IAEA drop tests. Subsequent studies<sup>3</sup> have shown that the puncture-resistance of concrete can be improved with more effective detailing of steel reinforcement. The use of certain metallic-based aggregates (e.g., ilmenite, magnetite, and hematite) is also effective.<sup>4,5</sup> In addition, steel fiber reinforcement improves a cask's resistance to impact and thermal loading, and polymer impregnation increases its impermeability to water.<sup>6</sup> Finally, an outer casing may be used to strengthen and protect the concrete wall. The casing may either be an outer steel liner which forms an integral part of the cask<sup>7</sup> or a reusable concrete or steel "overpack."<sup>7-8</sup>

## PROTOTYPE CASK DESIGN

The conceptual design of a full-size prototype cask, as formulated and investigated at Ontario Hydro, is shown in Fig. 1. Essentially, the cask consists of a sealed steel chamber within a reinforced concrete body. It is cylindrical in shape and has a storage capacity of two standard CANDU fuel-storage modules. The steel chamber, which lines the inner cavity of the cask, is a 25 mm (1 in.) thick carbon steel plate and forms the primary containment boundary for the irradiated payload. Irradiated fuel bundles are sealed in the inner cavity by welding a carbon steel lid to the chamber walls. The entrance to the cavity is then sealed with a concrete lid bolted to the main cask body. The space between the concrete lid and concrete walls is grouted to provide corrosion protection for the hardware and to insure even force distribution on impact. The cylindrical shape was chosen for better impact and pressure resistance, and the two-module capacity maintains the overall cask size within road transportation limits.

The cask is constructed of high-density, high-strength concrete. The 530 mm (21 in.) thick walls are rein-

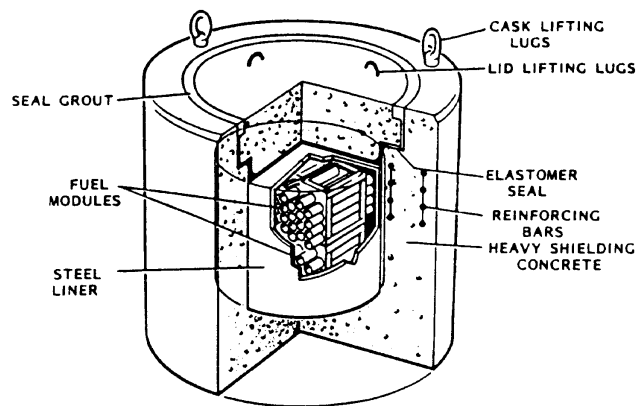


Fig. 1 — Conceptual drawing of concrete cask

forced with two layers of No. 20 bars at 120 mm (4¾ in.) centers in the circumferential direction, and two layers of No. 25 bars at 120 mm (4¾ in.) centers in the longitudinal direction. The overall dimensions of the cask include a 2750-mm (108-in.) diameter and a 2410-mm (95-in.) length; dimensions of the cavity are 1640 mm (65 in.) in diameter and 1300 mm (51 in.) in length. The dead weight, empty of fuel bundles, is 48,000 kg (52 tons).

## PERFORMANCE REQUIREMENTS

A prototype cask must undergo rigorous testing before it can be licensed for high-level waste transport. As part of the IAEA licensing requirements, a model must be subjected to two successive drops from different heights followed by a fire exposure. The guidelines for these tests<sup>9</sup> are as follows:

1. One drop test is to be a free drop from a 9-m (30-ft) height onto an unyielding surface. The cask orientation at impact must be such that the container is likely to sustain maximum damage.

2. Another drop test is to be a puncture test, where the cask is dropped from a 1-m (3.3-ft) height onto a vertical steel pin rigidly mounted to the unyielding surface. Again, the orientation is to be such as to inflict the greatest amount of damage. The recommended pin dimensions are 150 mm (6 in.) in diameter and 200 mm (8 in.) in length, but the actual dimensions are to be chosen so as to cause maximum damage.

3. The actual order in which the drop tests are conducted must be such that the cask will suffer the greatest damage upon completion of the drops.

4. The same model is then to be engulfed in a hydrocarbon fuel/air fire for 30 min. The average emissivity coefficient of the fire shall be 0.9 with an average flame temperature of 800 C (1470 F).

Upon completion of testing, the cask must be shown to have retained its structural and functional integrity. The pass/fail criteria are that the cask must maintain a specified level of radiation shielding and any loss of its radioactive contents must not exceed a specified maximum rate.<sup>9</sup> Under normal service conditions, the cask is expected to remain essentially crack-free, to meet very stringent IAEA radiation limits.

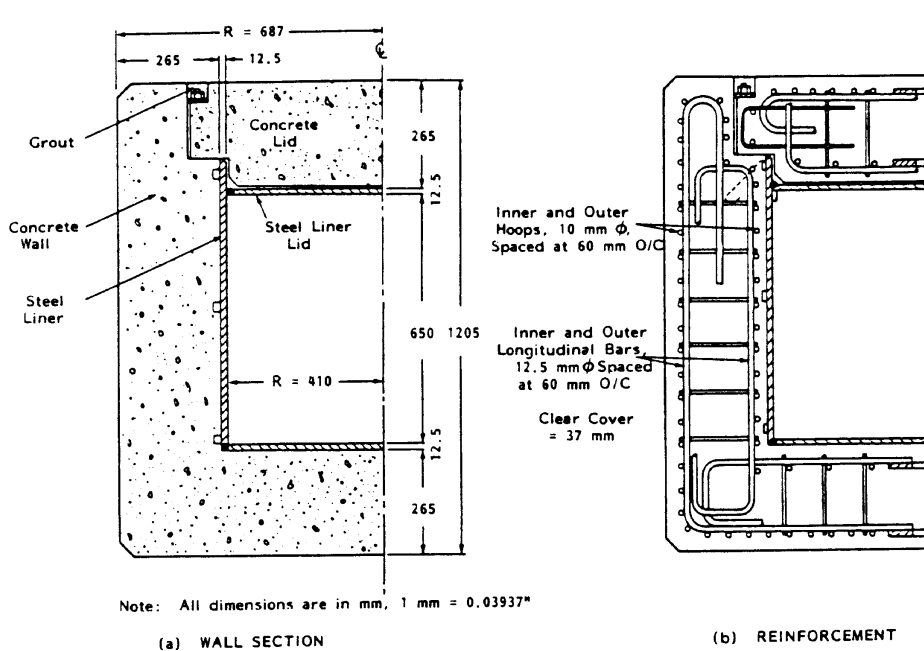


Fig. 2 — Details of half-scale model

Table 1 — Mix proportions and properties of fresh concrete\*

Cement <sup>1</sup>	Mix proportions (kg/m <sup>3</sup> )		Aggregates		Super-plasticizer, ml/kg	w/c	Slump, mm	Air, percent	Plastic density, kg/m <sup>3</sup>
	Silica fume	Water	Fine	Coarse <sup>2</sup>					
318	80	159	1289	1753	63.7	0.40	195	4.3	3599

\*From Reference 12: Proportions and properties given are those for the drop and fire test model. There was negligible variation for the second model.

<sup>1</sup>ASTM Type 5 — sulfate resistant.

<sup>2</sup>6 mm (0.25 in.) maximum.

NOTE: 1 kg/m<sup>3</sup> = 0.0624 lb/ft<sup>3</sup>; ml/kg = 1.53 U.S. fluid oz/100 lb.

Table 2 — Concrete properties

Compressive strength, MPa	62.9
Tensile strength, <sup>1</sup> MPa	4.7
Modulus of elasticity, MPa	58,900
Hardened density, kg/m <sup>3</sup>	3630
Thermal diffusivity, m <sup>2</sup> /s	0.091 × 10 <sup>-5</sup>
Coefficient of thermal expansion, degree C	11.25 × 10 <sup>-6</sup>

\*From Reference 13: Properties given are those for the drop and fire test model. There was negligible variation for the second model. Strength properties are at 28 days.

<sup>1</sup>Split cylinder test.

NOTE: 1 MPa = 0.145 ksi; 1 kg/m<sup>3</sup> = 0.0624 lb/ft<sup>3</sup>; 1 m<sup>2</sup>/s = 38,740 ft<sup>2</sup>/hr; °C = (°F - 32) ÷ 1.8.

## SCALE CONSIDERATIONS

The testing of scale models has proven to be an acceptable method for analyzing drop test response. Accurate relationships have been derived for the correlation of deflection, stress, force, energy, mass, time, and acceleration<sup>2</sup> provided linear geometric scaling is used and the impact velocity is the same for the model and prototype. These relationships have been confirmed by many tests of model casks with varying scale ratios. Not surprisingly, the correlation of results is best for models closer in size to the full-scale specimen. Minimum recommended scale values found in literature have ranged from 1/8 to 1/4.<sup>10-11</sup>

To correctly model reinforced concrete behavior, it is necessary to scale down the steel reinforcement and aggregate sizes, and to modify the cement mixture so that

the compressive failure stress of the scale model cement is the same as for the prototype cement.<sup>2</sup> For the steel reinforcement, both the bar diameter and the spacing must be scaled so that the same reinforcing ratios are maintained. Scaling of the concrete aggregates must be such that the mechanical and thermal properties of the concrete are maintained while the aggregate sizes are reduced.

For fire testing a scale model, the fire temperature and duration of exposure must also be modified. The changes are necessary to simulate the induced thermal loads and temperature distributions in the cask as they relate to structural response of the prototype. Similarly, the internal heat loads specified for simulating in-service design conditions must also be adjusted.

## HALF-SCALE MODEL

The half-scale models constructed had overall dimensions of 1205 mm (47.4 in.) in height and 1374 mm (54.1 in.) in outside diameter [see Fig. 2(a)]. The primary containment steel chamber was fabricated from 12.5 mm (0.5 in.) thick plate and had nominal dimensions of 650 mm (25.6 in.) in height and 820 mm (32.3 in.) in diameter. The concrete walls were 265 mm (10.5 in.) thick. The weight of the model, when empty, was approximately 6000 kg (6.6 tons).



Fig. 3 — Concrete cask model as built

Reinforcement details are shown in Fig. 2(b). The longitudinal reinforcement consisted of two layers of steel placed 47 mm (1.85 in.) from the outside and inside faces of the wall, with the bars spaced at 60 mm (2.4 in.) on centers. Similarly, there were two layers of circumferential reinforcement, placed 37 mm (1.5 in.) from the outside and inside faces of the wall, with the bars vertically spaced at 60 mm (2.4 in.) on centers. The longitudinal bars had a nominal diameter of 12.5 mm (0.5 in.) and the circumferential bars had a nominal diameter of 10 mm (0.4 in.).

The concrete used in the cask was of high-density, high-strength design. The high density, necessary for radiation shielding, was achieved using magnetite and hematite aggregates and arrived at 3630 kg/m<sup>3</sup> (226 lb/ft<sup>3</sup>). The entire range of aggregate sizes was a scaled version of the full-scale design mix. The coarse aggregate was a 6 mm (0.25 in.) maximum size magnetite and the fines were specularite hematite. A design strength of 45 MPa (6.5 ksi) was specified to give the cask good impact resistance and high energy absorbing capacity. Actual strengths in excess of 60 MPa (8.7 ksi) at 28 days were achieved using sulfate-resistant (ASTM Type 5) cement and silica fume, together with a superplasticizing admixture. The mix proportions and concrete properties are given in Tables 1 and 2, respectively.

Instrumentation for the first model included 2 triaxial accelerometers, 8 bar-mounted quarter-bridge strain gages, and 48 thermocouples for acceleration, strain, and temperature measurements, respectively. The second model was extensively instrumented with 66 strain gages and 42 thermocouples, generally located on two meridians.

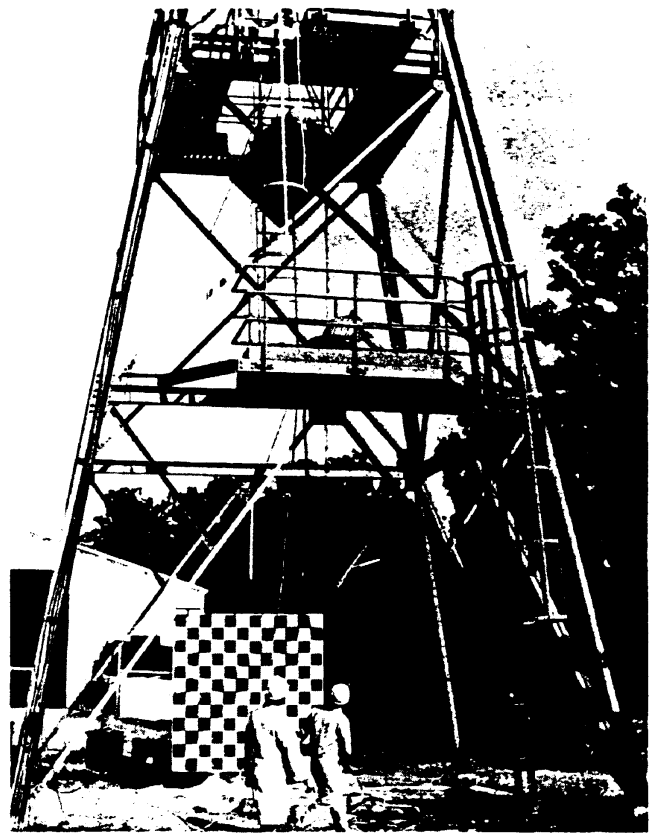


Fig. 4 — Cask model No. 1 in position for 9-m drop

The half-scale model, as constructed and prior to testing, is shown in Fig. 3. Full details of the model design, construction, and instrumentation can be found in References 14 and 15.

#### TEST PROGRAM — CASK MODEL NO. 1

Testing of the first model was conducted at AECL's Nuclear Laboratory at Chalk River, Ontario, which is equipped with a drop test facility and an open fire test pit that meet IAEA specifications. In implementing the IAEA guidelines, it was decided that the 9 m (30 ft) drop test should precede the puncture test in order to maximize damage.

For the first drop, 9 m (30 ft) onto an unyielding surface, the cask was oriented so it would impact on its upper edge (see Fig. 4). The cask's center of gravity was positioned above the impact point to minimize the energy loss due to rotational movement of the specimen after impact. This orientation was chosen in an attempt to damage the cask in the area of the concrete lid and sealing system, perceived to be the most vulnerable area.

For the 1-m drop onto a pin, the same cask orientation and impact point were chosen as for the 9-m drop (see Fig. 5). Again, the cask sealing system was the target of destruction. It was anticipated that the cask would have suffered extensive concrete loss from the initial impact and an attempt should be made to penetrate the concrete in this weakened zone. The pin used for the puncture test was 75 mm (3 in.) in diameter and

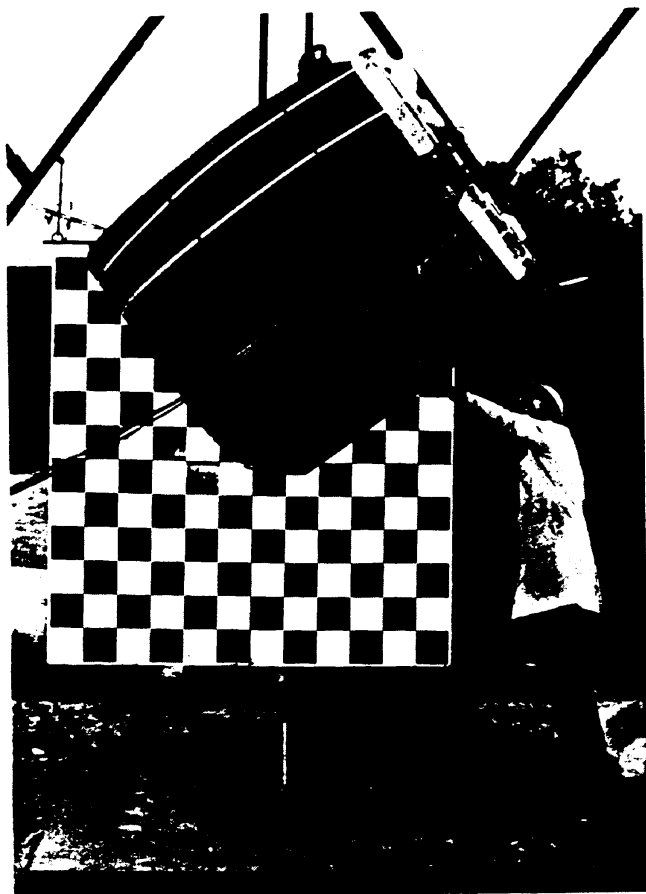


*Fig. 5 — Cask model No. 1 in position for 1-m drop onto steel pin*

280 mm (11 in.) in height. This size was selected on the basis that 75 mm (3 in.) is a half-scale diameter and 280 mm (11 in.) is the depth of the concrete to the steel chamber at the impact point.

The same model was then subjected to the fire test. A full-scale fire test requires exposure time of 30 min and a temperature of 800 C (1470 F). The theoretical equivalent for a half-scale model is a 7.5-min exposure to 971 C (1780 F).<sup>16-17</sup> Further, Reference 16 recommends the time be adjusted according to the flame temperatures actually recorded during the test to compensate for variable flame temperatures and emissivities. In the case of the half-scale concrete cask model, software problems resulted in flame temperatures above 500 C (930 F) not being recorded. Therefore, an exposure time of 10.5 min was arbitrarily chosen to compensate for the resulting uncertainty. Subsequent tests at Chalk River indicated an average flame temperature of 1000 C (1830 F), which would have required only a 7.5-min exposure.<sup>16</sup>

#### **TEST PROGRAM — CASK MODEL NO. 2**

The test program the second half-scale model was subjected to was designed to study the cask's response to realistic and diverse thermal environments. The program consisted of four distinct phases of tests: heat

transfer, power-cycling, accelerated weathering, and maximum heat-load tests. In each of these tests, the model was subjected to various combinations of internal heat load and ambient conditions. The internal heat loads were based on the decay heat of irradiated fuel of an age and quantity as that to be stored in the casks. The prescribed ambient conditions were those expected in the storage phase of IFM. The tests are described as follows.

In the heat transfer tests, the model cask was subjected to a constant internal thermal load and different, but constant, external ambient temperatures maintained until steady state conditions were achieved. The internal heat load was 750 watts, and the ambient temperature conditions ranged from 35 to -20 C (95 to -4 F). The objectives were to monitor the induced thermal gradients in the cask wall, and to study the cask's heat dissipation characteristics under various ambient conditions.

In the power-cycling tests, the cask model was subjected to a constant ambient outside temperature while the internal heat load was ramped through a series of on-off cycles. In all, the cask was subjected to five power cycles of 750 watts while the external ambient temperature was maintained at -20 C. Power was switched on or off only after the thermal gradients had stabilized. This test was meant to assess the cask's behavior under shock loading events, which in practice would occur when a cask is loaded or unloaded with fuel.

In the accelerated weathering tests, the cask model was subjected to a constant internal thermal load of 213 watts and alternating freezing and thawing temperatures externally. The internal heat load was that of 30-year cooled fuel and the external ambient temperature was cycled between -18 and 4 C (0 and 40 F) for 22 complete cycles. Freeze-thaw actions were simulated by spraying water on the surface of the specimen. The purpose of this test was to determine the effects of variable exposure.

The intent of the maximum heat load test was to subject the model to internal heat loads greater than 750 watts, while the outside ambient temperature was cycled between temperatures of 20 and -20 C (68 and -4 F). The internal heat loads started at 1.0 kW and increased to a value of 1.5 kW after one complete cycle of the ambient temperature.

All tests were conducted in a variable condition room, which had a temperature range of -20 to 35 C (-4 to 95 F) and a relative humidity range of 25 to 75 percent. The decay heat was simulated by placing an electric heater in the cask's steel chamber. The electric heater consisted of an annular vessel, similar in shape to that of a scaled-down fuel basket, with heating elements placed around its circumference. The heater output was controlled with a variable voltage regulator and the supplied power (wattage) was continuously recorded using a strip chart watt meter. The heater had a rated maximum capacity of 1.5 kW.

Note that the internal heat loads of 750 and 213

watts correspond to full-scale design loads of 3000 and 850 watts, respectively. A decay heat output of 3000 watts is that of a 5 year cooled fuel, and 850 watts is that of a 30 year cooled fuel. The values of 1.0 kW and 1.5 kW are arbitrarily selected heat loads greater than design values, which correspond to full-scale loads of 4.0 kW and 6.0 kW, respectively. The equivalent heat loads for the half-scale model were calculated on the basis of achieving the same thermal gradient through the model wall as that which would occur in the full-scale prototype.

### RESULTS FROM 9-m DROP TEST

Upon impact, the cask rolled approximately 10 deg counterclockwise, but otherwise did not bounce. The orientation of the cask's center of gravity above the impact point, at the time of impact, was approximately 2 deg off vertical. The peak deceleration, on the outside of the cask and inside the steel chamber, was essentially the same at 118 and 115 g, respectively (see Table 3).

The cask experienced significant loss of concrete at impact. Fragments of concrete as large as 50 mm (2 in.) in diameter were projected as far as 10 m (33 ft) from the impact point. Although the total amount of concrete lost was less than 1.5 percent of the cask's entire weight, the loss was concentrated in the two areas centered about the 0 deg (impact) and 180 deg meridian, as can be seen in Fig. 6. There was no spalling or cracking in areas 90 deg from the impact point. The loss of concrete at the 0 meridian extended over a circumferential distance of 90 deg and an average of one-quarter of the cask's height. The top outer hoop bars were twisted and bent, two longitudinal reinforcing bars at 0 and 354 deg were ruptured, and the top interior hoop bar was severely bent. At 180 deg from the impact point, the concrete loss and exposed reinforcing bar were confined to the top shoulder of the cask, from which a large network of cracks extended part way along the cask's length. A major crack 19 mm (0.75 in.) wide was located at the 200 deg meridian, across which three of the top outer hoop bars were ruptured. At approximately 22.5 deg on either side of the 0 deg meridian, the concrete lid had separated from the cask wall. The resulting gaps were approximately 6 mm (0.25 in.) wide. The lid movement is confirmed in Fig. 6 by examining the grid line dividing sector 7 and 8. The grid line on the concrete lid is offset towards the 180 deg meridian with respect to the corresponding line on the cask wall. This offset was approximately 10 mm (0.4 in.).

Strain measurements from the 9-m drop are reported in Table 4. The maximum tensile strain of the reinforcing steel measured at the eight instrumented locations was 1200 microstrain and occurred in the hoop bar nearest the impact point. This bar, an interior hoop located approximately 220 mm (9 in.) below the top of the cask, was the inner counterpart of one of the outer bars that had ruptured. The maximum measured longitudinal compressive strain occurred closest to the im-

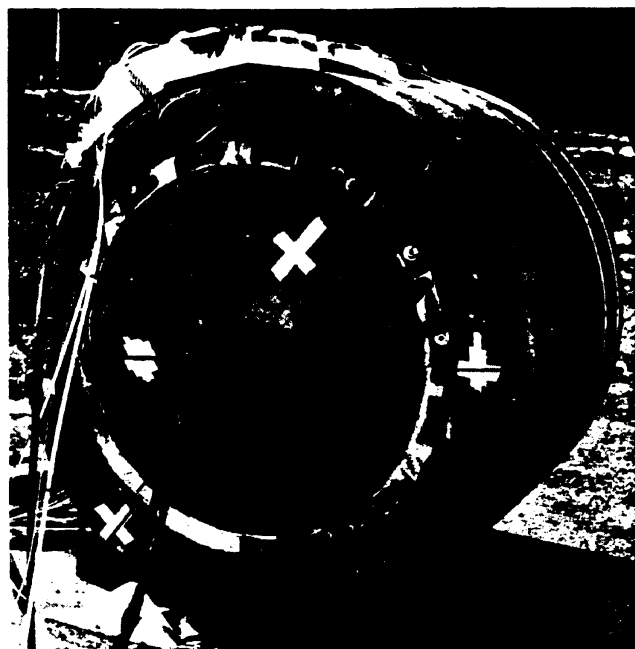


Fig. 6 — Cask model No. 1 after 9-m drop

Table 3 — Maximum accelerations

Drop	Acceleration g					
	Longitudinal direction		Parallel to lid		Vertical direction	
	Outside	Inside	Outside	Inside	Outside	Inside
9 m	74.2	70.9	92.4	90.8	118.4	114.7
1 m	15.9	12.1	12.3	17.5	19.4	21.2

Table 4 — Maximum reinforcing bar strains

Strain gage	Location	Bar type	Strain $\mu\epsilon$	
			9-m drop	1-m drop
1	220 mm below top end inner layer of steel	hoop	+ 1200	- 66
2	220 mm below top end inner layer of steel	longitudinal	- 840	- 152
3	600 mm below top end inner layer of steel	hoop	+ 288	- 14
4	600 mm below top end inner layer of steel	longitudinal	- 510	- 60
5	600 mm below top end outer layer of steel	hoop	+ 80	+ 18
6	600 mm below top end outer layer of steel	longitudinal	- 200	- 28
7	950 mm below top end inner layer of steel	hoop	+ 144	+ 20
8	950 mm below top end inner layer of steel	longitudinal	- 96	- 22

point and attained a value of -840 microstrain. All strains recorded during the 9-m drop were below the yield values for the bars. Obviously, however, some reinforcing bars exceeded yield strain at unmonitored locations, as evidenced by the ruptured bars. A complete discussion of test observations and data can be found in Reference 14.

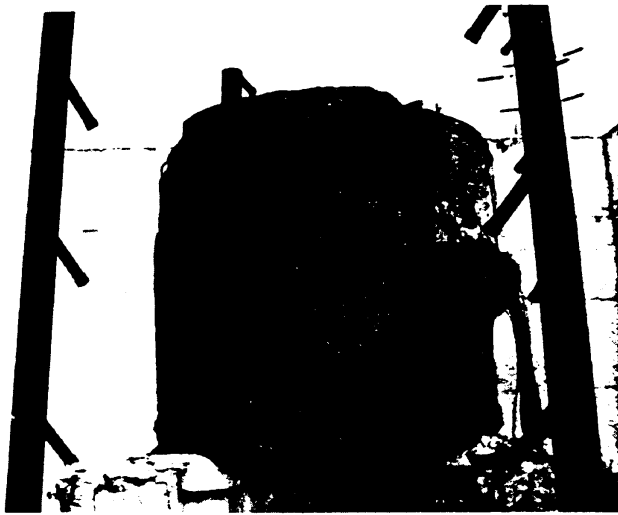


Fig. 7 — Cask model No. 1 after fire test showing damage on windward side

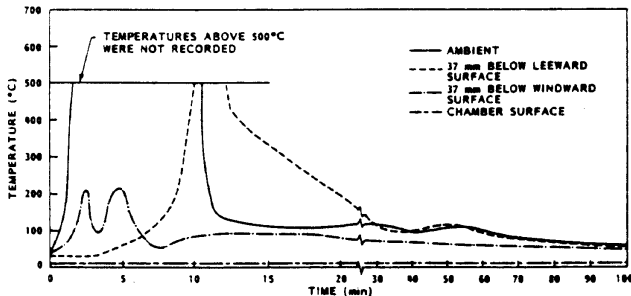


Fig. 8 — Thermal conditions during fire test

### RESULTS OF PIN DROP TEST

The 1 m (3.3 ft) pin drop test followed the 9-m (30-ft) drop. This test was unsuccessful at inflicting additional damage to the cask because, at impact, the steel pin was bent and partially torn away from the base plate. The steel pin did not penetrate the outer layer of reinforcing bars, and an inspection of the cask did not disclose any new cracks or significant additional spalling. Some concrete loss occurred when the cask glanced off the pin and impacted on the target surface. Accelerations and reinforcement strains recorded during the pin drop test are also given in Tables 3 and 4.

### RESULTS OF FIRE TEST

The principal damage caused by the fire was spalling of surface concrete (see Fig. 7), which began after approximately 5 min of fire exposure. The spalling was a continuous process, as small fragments of concrete 10 mm (0.4 in.) maximum diameter were projected from the cask surface. No new cracks developed on the surface, nor was there evidence that the original cracks from the drop tests had widened significantly.

On the day of the fire test, a breeze prevailed towards the open front doors of the fire pit. This breeze resulted in an uneven flame distribution around the

cask and, consequently, in differences in the thermal gradients recorded on the windward and leeward faces of the cask. The maximum gradient recorded through the wall on the leeward side was 386 C (725 F). This gradient was extremely nonlinear, as the temperature was 400 C (750 F) 37 mm (1.5 in.) below the concrete surface, 30 C (86 F) at middepth of the wall, and 14 C (57 F) at the surface of the steel liner. The corresponding gradient on the windward face was only 146 C (295 F). The temperature 37 mm (1.5 in.) below the surface was 160 C (320 F), at middepth 20 C (68 F), and 14 C (57 F) on the steel liner. The resulting fire damage was consistent with the uneven flame distribution as the maximum spalling was sustained on the leeward face and very little spalling occurred on the windward face. The maximum depth of spalling on the leeward side was approximately 50 mm (2.0 in.) or 19 percent of the concrete wall thickness.

Thermocouple readings indicated that the concrete body was effective in shielding the chamber and payload from the fire. The ambient temperature in the vessel, initially 14 C (57 F), remained stable for 30 min before slowly rising (see Fig. 8). At 90 min, the internal temperature had peaked at only 16 C (61 F).

### RESULTS OF THERMAL TESTS

Thermal load conditions imposed on the second test model and the resulting thermal gradients are shown in Fig. 9. The response curve for Thermocouple T42 represents the temperature in the variable condition room, while Thermocouple T37 gives the internal temperature of the steel chamber. Thermocouple T39 was located on the exterior surface of the concrete wall; Thermocouple T10 was located 47 mm (1.85 in.) below the exterior concrete surface; Thermocouple T11 was located 237 mm (9.33 in.) below the exterior surface; and Thermocouple T12 was located on the interior surface of the steel liner.

During the heat transfer test [Fig. 9(a)], a maximum temperature of 75 C (167 F) was attained inside the chamber when the outside temperature was 35 C (95 F). Approximately 72 hr were required to achieve stable thermal gradient conditions after each change in the outside temperature. The maximum temperature difference across the wall was 17 C (31 F), and this occurred equally through the entire range of outside temperatures. Also note the significant temperature differential between the chamber wall (T12) and the chamber air (T37), indicative of the so-called skin effect. The maximum air temperature was 75 C (167 F), while the maximum temperature of the steel wall was 50 C (122 F). Similar observations can be made with respect to maximum thermal gradients and time required to achieve stable conditions in the power cycling test [Fig. 9(b)], accelerated weathering test [Fig. 9(c)], and maximum heat load test [Fig. 9(d)]. Further, in the power-cycling test with the ambient temperature at -20 C, the freezing front penetrated to approximately three-quarters of the depth of the concrete cask wall. During the

accelerated weathering test, under the coldest conditions, the freezing front completely penetrated the wall. The most severe thermal conditions were achieved during the maximum heat load test, where a thermal gradient of 34 C (60 F) and a chamber temperature of 98 C (208 F) were attained.

Crack patterns were monitored and crack widths were measured at frequent intervals during the thermal tests. Several hairline cracks existed prior to the testing, a likely result of drying shrinkage. The heat transfer, power-cycling, and accelerated weathering tests did not cause any new cracks to form or any existing cracks to propagate or widen. The maximum heat-load test did, however, cause further cracking with a maximum crack width of 0.2 mm (0.008 in.) observed. At the conclusion of the test, many of the new cracks were no longer visible to the naked eye, and the existing cracks had generally returned to their original widths.

Fig. 10 shows the strains measured on the outside and inside layers of the circumferential reinforcement. During the heat-transfer test [Fig. 10(a)], compressive strains were induced in the inner hoops while tensile straining occurred in the outer hoops. Similar trends occurred during the power-cycling [Fig. 10(b)] and accelerated weathering tests [Fig. 10(c)], although the various thermal conditions resulted in somewhat differing patterns. Peaks in the strain response typically coincided with a change in boundary temperature (e.g., turning heater on or off). In general, the maximum tensile strains recorded during the first three tests were well below 100 microstrain (i.e., concrete cracking strain). Strains recorded during the maximum heat load test [Fig. 10(d)] were much higher, however. Further, the inner hoop reinforcement showed significant tensile strain as a cumulative result of the temperature cycling. With high tensile strains occurring simultaneously in the outer layer of reinforcement, the indication is that cracking was induced through the total thickness of the cask wall.

Complete data and a detailed discussion of the test results can be found in Reference 15.

## CONCLUSIONS

The following conclusions can be drawn from the impact and fire tests conducted on the first model:

1. The cask had maintained its structural integrity at the conclusion of testing. The reinforced concrete body proved effective in protecting the steel payload chamber from the high impact forces in the drop tests and from the extreme heat in the fire test. Inspection of the liner revealed that no tearing or distortion had occurred, and that the chamber remained leak-tight.

2. The structural system exhibited good energy-absorbing capacity. The peak deceleration at impact was relatively low at 118 g, and the cask did not bounce at impact. The payload chamber did not experience a different deceleration from the cask body at impact.

3. Significant cracking occurred as a result of the 9-m (30-ft) drop, in a region of the cask 180 deg from the

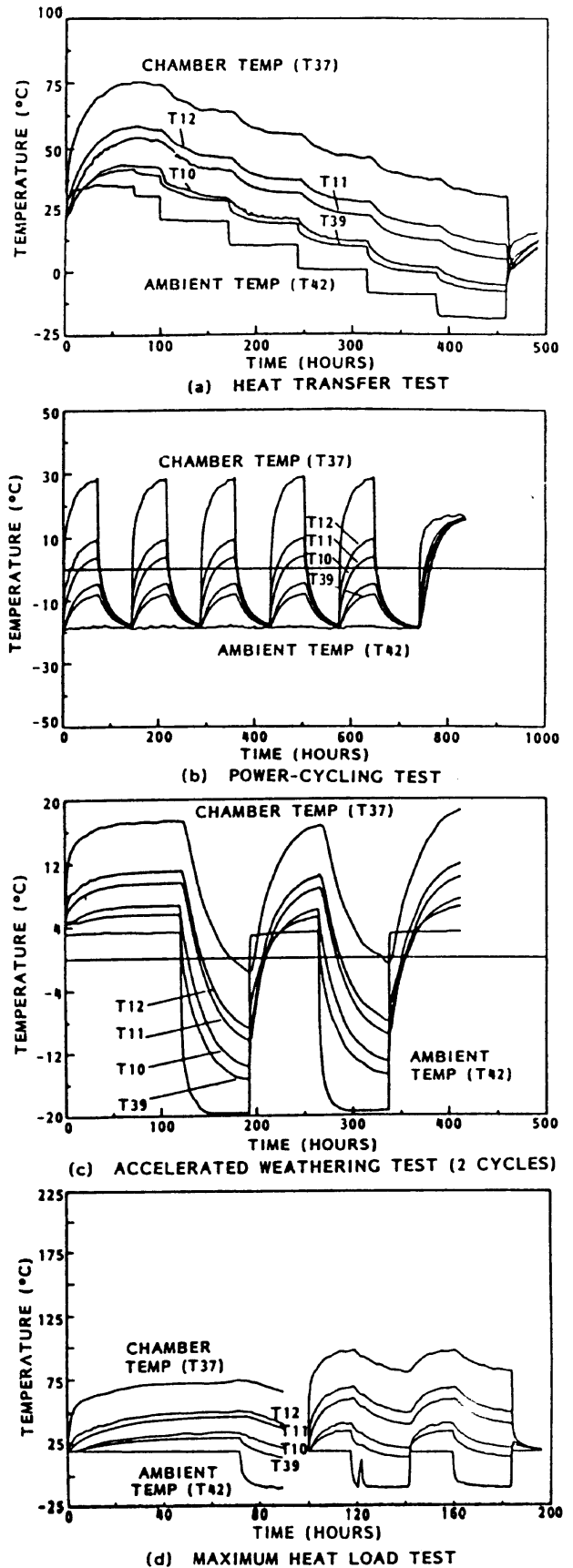


Fig. 9 — Thermal load conditions imposed during testing of cask model No. 2

impact point. These cracks were caused when the concrete lid was forced back into the 180 deg hemisphere at impact. Rupturing of some reinforcing hoops also



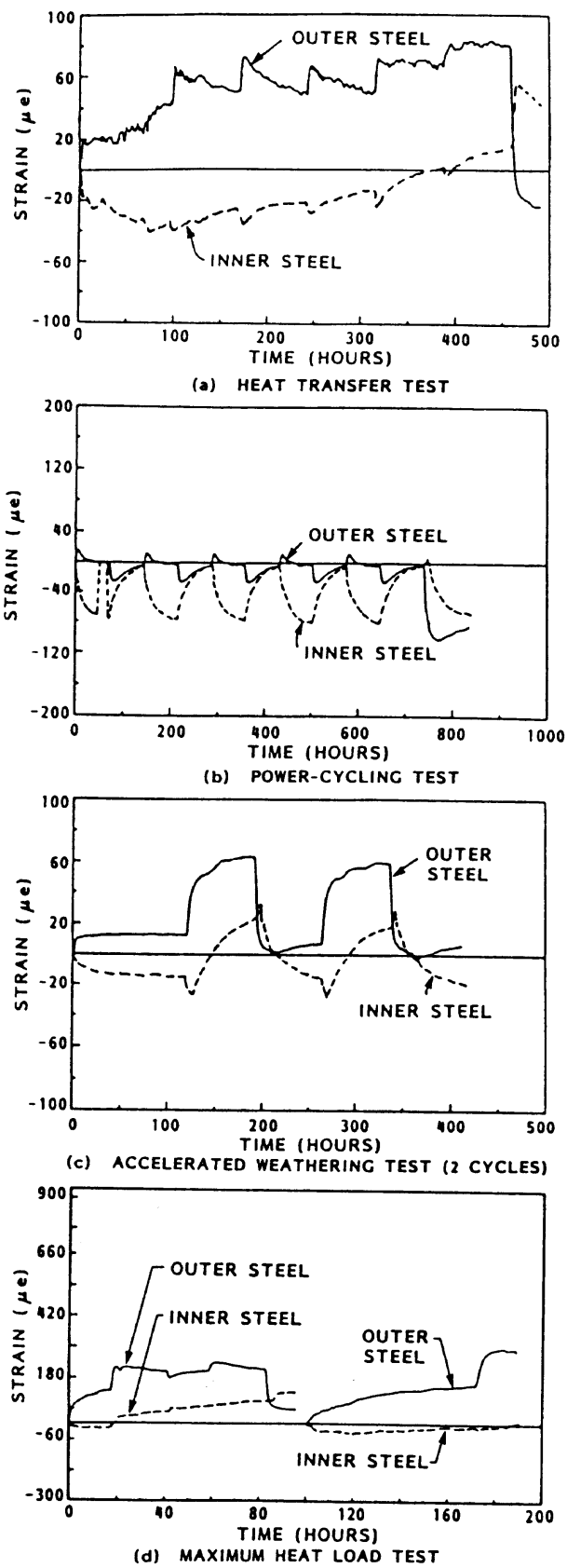


Fig. 10 — Strains in hoop reinforcement of cask model No. 2

took place in this region. It is evident that a higher percentage of reinforcing hoop steel is required to resist the high tensile stresses due to the oblique corner drop.

4. Significant crushing and spalling of concrete also occurred as a result of the 9-m (30-ft) drop. The damage was concentrated at the impact point and directly across on the lid surface. The total amount of concrete lost was less than 1.5 percent of the cask's weight, however. There was no cracking or spalling in areas 90 deg from the impact point.

5. The 1-m (3.3-ft) drop onto a pin did not result in any further significant damage to the cask. The pin did not penetrate past the outer layer of reinforcing bars, indicating the high density concrete together with proper detailing provided adequate puncture resistance.

6. Significant damage to the cask occurred during the fire test, in which there was continuous spalling of the concrete. Maximum cumulative concrete losses from the drop and fire tests were 19 percent of the wall thickness in local areas.

7. The extremely nonlinear temperature gradients through the thickness of the wall and circumferentially around the cask did not cause any new cracks to open or existing cracks to widen on the exterior surface.

8. The concrete walls effectively protected the steel chamber from extreme rises in temperature. The ambient air temperature of the chamber rose by only 2 C as recorded after a 10.5 min exposure to 1000 C (1832 F) and an 80 min cool-down period.

The following was concluded from the thermal tests conducted on the second model:

1. The high-density concrete did not suffer any apparent degradation as a result of the exposure to variable ambient temperatures and humidity, and to repeated freeze-thaw cycles. No evidence of spalling, pitting, or other form of surface deterioration was visible.
2. The model withstood the initial three thermal tests, which were based on design service conditions, without spalling or cracking. The measured tensile strains in the reinforcement remained below concrete cracking strain levels, and all strains were recoverable at the end of the tests.

3. For a given internal heat load, the thermal gradient achieved was constant, irrespective of the external ambient temperature.

4. Under heat loads greater than design service conditions, significant surface cracking was observed. Tensile strains measured on both the inside and outside reinforcement indicated the cracks penetrated the complete wall thickness.

#### ACKNOWLEDGMENTS

The test programs reported in this paper were fully funded by and partially conducted at Ontario Hydro. The drop and fire tests were conducted at AECL's Chalk River Nuclear Laboratories. The authors wish to express their sincerest appreciation for the support received.

#### REFERENCES

1. Ohta, M. M., "The Concrete Canister Program," Report No. AECL-5965, Atomic Energy of Canada Limited, Feb. 1978, 56 pp.

2. Merrett, G. J., "Scale-Model Testing of a Concrete Canister," *Report No. WNRE-452*, Atomic Energy of Canada Limited, Dec. 1980, 50 pp.
3. Zerna, W.; Schnellenbach, G.; and Stangenberg, F., "Optimized Reinforcement of Nuclear Power Plant Structures for Aircraft Impact Forces," *Nuclear Engineering and Design* (Lausanne), V. 37, 1976, p. 313.
4. Mentès, G. A., and Mammoliti, F., "Report on Visit to the Whiteshell Nuclear Research Establishment," *D D Report*, Ontario Hydro, Toronto, May 1983, 5 pp.
5. Laug, R., and Lührman, A., "Stability of a Special High-Density Concrete as a Material for Spent Fuel Shipping and Storage Casks," *Proceedings*, 6th International Symposium on Packing and Transportation of Radioactive Materials, West Berlin, Nov. 1980, pp. 249-253.
6. Arakly, K.; Maki, Y.; Shinji, Y.; Ishizaki, K.; Minegishi, K.; and Sudoh, G., "PIC Container for Containment and Disposal of Low and Intermediate Level Radioactive Wastes," *Report No. JAERI-M9380*, Japan Atomic Energy Research Institute, Mar. 1981, 13 pp.
7. Pearsall, S. G.; Majeski, S.; and Gemmel, L., "Design and Testing of a Shipping Container for Large Quantities of Radioactive Waste," *Proceedings*, 2nd International Symposium on Packaging and Transportation of Radioactive Materials, Gatlinburg, Oct. 1968, pp. 624-631.
8. Goetsch, S. D., and Thomson, J. D., "FFTF Disposable Solid Waste Cask," *PATRAM 83*, 7th International Symposium on Packaging and Transportation of Radioactive Materials, New Orleans, May 1983, pp. 1201-1208.
9. "Regulations for the Safe Transport of Radioactive Materials," *Safety Series No. 6*, International Atomic Energy Agency, Revised Edition, 1973, 18 pp.
10. Shappert, L. B.; Evans, J. H.; and Stoddart, W. C., "Methods of Determining Compliance of Type B Packages with the Thermal and Mechanical Regulatory Requirements," *Proceedings*, International Atomic Energy Agency, Vienna, Feb. 1971, pp. 487-507.
11. Aoki, S., "Tests on a Spent Fuel Shipping Cask in Japan," *Proceedings*, International Atomic Energy Agency, Vienna, Feb. 1971, pp. 539-547.
12. Hooton, R. D., "Concrete Integrated Cask Program: Development of High Strength, High Density Concrete Mixes," *Research Division Report No. 85-132-H*, Ontario Hydro, Toronto, 1985, 30 pp.
13. Mukherjee, P. K., "Concrete Integrated Cask Program: Thermal Properties of High Density Concrete," *Research Division Report No. 85-234-H*, Ontario Hydro, Toronto, 1985, 42 pp.
14. Sato, J. A., and Vecchio, F. J., "Concrete Integrated Cask Program: Structural Testing of a Half-Scale Model," *Research Division Report No. 85-64-H*, Ontario Hydro, Toronto, 1985, 43 pp.
15. Sato, J. A., and Vecchio, F. J., "Concrete Integrated Cask Program: Thermal Testing of a Half-Scale Model," *Research Division Report No. 86-59-H*, Ontario Hydro, Toronto, 1986, 47 pp.
16. Watchell, G. P., "Drop and Fire Tests of Half-Scale Model of TN-9 Shipping Container," *Proceedings*, 4th International Symposium on Packaging and Transportation of Radioactive Materials, 1974, pp. 244-260.
17. Watchell, G. P., "Can We Model a Fire Test?," *Proceedings*, International Symposium for Packaging and Transportation of Radioactive Materials, *Report No. SC-RR-65-98*, Sandia Laboratories, Albuquerque, 1965, pp. 133-140.